Study of atomic excitations in sputtering with the use of Mg, Al, Ca, and Cd targets

E. Veje
Physics Laboratory II, H.C. Ørsted Institute, Universitetsparken 5, DK-2100 Copenhagen, Denmark
(Received 20 September 1982; revised manuscript received 1 March 1983)

Solid targets of Mg, Al, Ca, and Cd have been bombarded with 80-keV Ar^+ ions. Photon emission from sputtered particles has been measured and converted to relative level populations. The experimental results are discussed in terms of a set of basic considerations outlined for atomic excitations in sputtering processes.

I. INTRODUCTION

This work is a continuation of our attempts[1-3] to systematically study atomic excitation in sputtering processes. A variety of models has been proposed for atomic excitation in sputtering processes. Some of them are referred to and discussed in Refs. 1–4. Also, Kelly[5,6] has recently reviewed the various models critically and concluded that of all models proposed, only a so-called statistical model,[6] based on a binary atomic-collision picture, gives a reasonable description. On the other hand, the so-called electron-pickup model[1-3] has been used to explain some experimental findings which seem to be difficult[2,3] to incorporate in the statistical model.[6]

In this paper we shall not argue at length for or against either (or any other) model. For such discussions, as well as for references to previously proposed models, the reader is referred to Refs. 1–6, especially Ref. 3. Rather, we shall first present a set of basic considerations for the excitation of sputtered species. Then, in later sections, experimental results are presented and discussed in terms of these considerations.

Throughout this paper we shall primarily be concerned with sputtering from clean, polycrystalline or amorphous elemental targets, oriented with the target surface perpendicular to the beam axis, but phenomena related to oxygenated target surfaces will also be discussed.

II. BASIC CONSIDERATIONS

When a swift, atomic projectile penetrates into a solid target, some of the target atoms initially located close to the projectile trajectory, will be set into motion, and one or more of these moving atoms may leave the solid as sputtered particles.[7] The sputtered atoms are initially bound close to, or at, the surface. The atomic bonds in the target are caused in one way or another by the valence-shell electrons, and various types of bonds exist, of which the metallic[8] and the covalent[8] bonds are of primary interest here because attention is focused on clean, elemental targets. However, an expansion of this discussion to also include ionically[8] bound systems seems to be straightforward.

A theoretical treatment as well as a qualitative model for visualizing atomic excitation in sputtering shall describe how one (or more) of the electrons from the valence band of the solid during the sputtering follows an atom and finally ends up in some free atomic eigenstate of the sputtered particle. Thus the initial state is a valence-band orbital of the solid, and the final state is a free atomic orbital. The excitation is a result of the evolution in time from the initial to the final state. In passing we note that the valence-shell electrons for atoms sputtered in their ground state undergo a time evolution similar to those for excited atoms, the only difference being that the final state is the ground state rather than an excited state. But the initial state is the same.

When dealing with electronic excitation in sputtering processes in which the target surface plane is perpendicular to the beam axis, one only needs to be concerned essentially with what happens to the valence electrons. Atoms sputtered with inner-shell excitations are rare, primarily because the inner-shell electrons are so tightly bound that they are only excited in rare, violent collisions. Furthermore, of the few inner-shell vacancies created during a collision cascade, most of them will become refilled before the atom is sputtered, owing to the short mean life of an inner-shell vacancy. Naturally, the situation will be different if the angle of incidence of the incoming beam is changed. For large angles of incidence, a projectile may knock out a target atom in one close collision. Inner-shell vacancy-creation probabilities may be large for such collisions, so that inner-shell excitations may well occur for large angles of incidence. However, inner-shell excitations are then created in almost binary atomic collisions and should consequently be treated as the outcome of such interactions.[9]

As described above, the final excitation is a result of the evolution in time from the initial electronic state in the solid to the final state in a free atom. Such an evolution in time is schematically demonstrated in Fig. 1, which shows the electronic energy structures of a typical metal (to the left of Fig. 1) and of a free atom or ion (to the right of Fig. 1). During the evolution in time, level broadenings and shifts will occur. They will depend on the actual choice of target element and are accordingly not shown specifically in Fig. 1.

The electronic structure of a solid exposed to heavy ion bombardment may, locally around the projectile trajectory, well be quite different from that of an undisturbed solid. Several atoms are set into motion during a collision cascade, and the changes in time of the internuclear distances will naturally change the electronic energy properties of the solid locally around the sputtering site. Most presumably, a broadening of the valence band will occur. Williams has suggested[10] that the term "work function" be dropped from sputtered ion discussions in favor of something like the "local surface potential barrier height" so that models which discuss the latter will not continue to be tested by experiments which measure the former. Regrettably, the actual initial electronic structure of

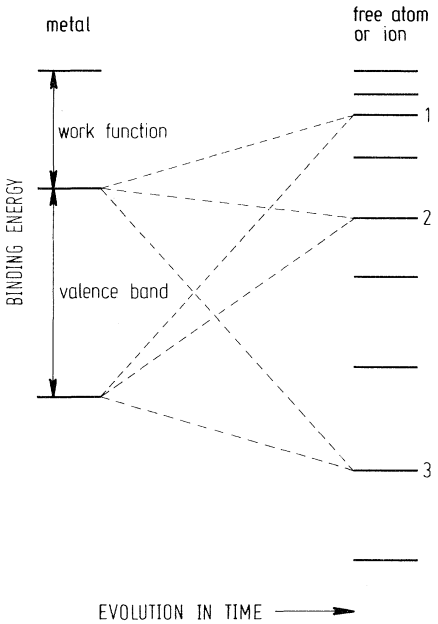

FIG. 1. Schematic representation of the binding-energy properties for a typical solid metal (to the left) and for a free atom or ion (to the right). Excitation in sputtering results from the evolution in time from the left to the right. A process leading to a final level like the one labeled 2 can be resonant, whereas processes leading to levels like those labeled 1 and 3 are off-resonant; see text.

relevance for atomic excitation in sputtering is unknown, and therefore, the electronic structure of an undisturbed solid has been used in previous discussions. This will also be the case in this paper due to lack of more realistic knowledge. The problem concerning local work-function determination is also illustrated in a recent theoretical work on photoemission by Lang and Williams.[11] They concluded that photoemission from inert-gas atoms adsorbed on surfaces can be used as an analytical tool for determination of the work function appropriate to microscopically small regions of a surface.

The bonds between the atoms in the solid are caused by the valence-shell electrons. The electronic structure of the solid will become excited when the projectile passes through it. This is what causes the electronic energy loss of the projectile, and is a source for secondary electron emission. For a metal, the relaxation time of the conduction electrons is short (around 10^{-19}—10^{-15} s) compared with the evolution in time of the collision cascade leading to sputtering. Thus that fraction of the energy of the projectile which is spent in exciting conduction electrons is immediately shared by a very large number of electrons. But for insulators, the lifetimes of excited electronic states are comparable to,[4,10,12] or maybe even larger than, the time of the collision cascade. Most of the sputtered particles will leave with relatively small kinetic energies late in the evolution of the collision cascade; only a few, swift atoms may leave early. Thus, for metals, the electronic structure will have relaxed to a fairly large extent when most of the sputtered atoms leave the solid, whereas for insulators, the electronic structure may well stay excited during the sputtering.

For metals, the Sommerfeld picture[13] may be applied as a crude starting point, i.e., the atoms are sitting as ionic cores immersed by an electron gas, made up of the valence electrons of the initially free atoms. In the solid metal, the mean free path of the valence electrons is large compared with the lattice spacing. The motion of an electron is delocalized.

In a covalent bond, the atoms in the solid tend, in a sense, to fill up the originally empty valence-shell orbitals by sharing electrons with neighboring atoms. Thus, loosely speaking, the electrons will initially be in orbits which are very similar in shape to those of the ground state of a free atom. Consequently they will be able to adjust continuously their motions adiabatically so that they end up in the atomic ground state, and very little or essentially no excitation will be observed in sputtering. This has been discussed in Ref. 3 in detail, and the discussion shall therefore not be repeated here.

In a pure metal, the valence-shell electrons will initially be delocalized, moving in a more or less uniform, average potential, as just described. On the way out, when passing through the surface, two fairly strong forces will act upon them, one being caused by the change in the potential, and the other being the attractive force from the core of the atom being sputtered. The potential energy for an electron inside the metal is numerically on the order of the sum of the work function and the Fermi energy ($\simeq$10 eV), whereas it is zero outside. The change takes place over a distance of approximately 1 nm. Therefore, the average electric field experienced on the electron when it passes through the surface will be of the order of 10 V/nm $=10^{10}$ V/m. This is the average electric field strength related to the potential step at the target surface, and it is a strong field. At the same time the electron will also feel an attractive force towards the core of the atom being sputtered. The field strength at the site of the electron, caused by the net charge of the core of the atom being sputtered, is roughly on the same order of magnitude, depending naturally on the average distance between the electron and the core center, as well as on the actual value of the core charge. Thus the field strength due to the potential change across the target surface cannot be regarded as only a fairly small disturbance of the valence electron(s) of the atom being sputtered. Therefore, a perturbation treatment will be inappropriate. Any valence-shell orbital and/or outer-shell orbital will not become established as a free, atomic eigenstate until the atom has moved some nanometers away from the solid, where the surface field has become reduced so much that it does not appreciably disturb the atom any longer. Additionally, we mention that the surface field at large distances from the surface may well be fairly weak, but on the other hand, it may well be fairly long ranging as a weak field, implying that the sputtered atom can be exposed to Stark effect mixings while the outer electrons are adjusting themselves into some atomic eigenstate. For treating the long-range Stark effect mixing, a perturbation treatment may suffice.

Electron-electron interactions will in many cases be fairly small during a sputtering event compared with the two above-mentioned fields. This means that, as a starting point, an independent-electron picture can be applied, ig-

noring the mutual electron-electron repulsions. This is a situation similar to the independent-electron picture for beam-foil excitations.[14] It will imply that no electron correlations will be created during the sputtering event, and also that possible electron correlations, like spin alignments, which existed in the solid in the remote past will pass preserved.

As described above, excitation in sputtering is a result of the evolution in time from an initial, valence-band state, to the final atomic state. For metal atoms this evolution can be visualized[1,2] as an electron pickup from the valence band to the atom being sputtered. Therefore, insight into the excitation process may, with some precaution, be gained by adapting the results from the theory of charge exchange in atom-atom collisions. Olson has recently found[15] that an electron will try to preserve its original orbital energy as well as the orbital size in an electron capture process. By adapting these two findings to sputtering events, one would expect that the population will be favored for final atomic states which have binding energies equal to or close to the binding energies of the valence electrons in the solid (i.e., a level like the one labeled 2 in Fig. 1), whereas final states which demand a relatively large amount of binding energy exchanged between the electron in question and the nuclear motion will be less populated. Note that this should apply not only for final states bound less than the initial state (a level like the one labeled 1 in Fig. 1), but also for final states bound *more tightly* (a level like the one labeled 3 in Fig. 1). The result is in agreement with the basic idea behind the Franck-Condon principle for molecules, which says that a coupling between electronic and nuclear motion is an unlikely process. In addition to this energy matching, final atomic states whose wave functions have good geometrical overlaps with the initial wave function will also presumably be preferentially populated. We must realize that there are two different conditions for preferential excitation. The resultant distribution of excitation upon different excited states will most presumably be a compromise between them, similar to what Olson found[15] for atom-atom collisions.

The kinetic energy distributions of sputtered, excited atoms have been (and still are) a great concern. Neither Doppler broadening data nor spatial distribution measurements yield unambiguous results, see, e.g., Refs. 5 and 6 and references cited in Ref. 16. Recently, however, Yu *et al.*[16] using a Doppler-shift laser fluorescence technique have directly demonstrated that for sputtered Ba atoms with excitation energies of 1.2 and 1.4 eV, and of electronic configurations completely different from that of the ground state, the most probable kinetic energies are comparable to those of sputtered ground-state atoms, and there are no kinetic energy thresholds. Although the energy distributions for excited atoms are broader than for ground-state atoms, there are no marked differences between the kinetic energy distributions for atoms excited to different levels. This is in itself a very important finding, because it demonstrates that atomic excitation in sputtering is not necessarily restricted to atoms with large, final kinetic energies. On the other hand, Yu *et al.*[16] measured on low-lying excited levels, whereas the spatial distribution measurements concern higher-lying levels. This makes a crucial difference between the two data sets, and further measurements are needed to clear up the situation. Anyway, it must be remembered that the atom being sputtered is initially bound to the solid. Therefore, initially it must have a kinetic energy larger than the binding energy. Thus in the early stages of the sputtering process the atomic kinetic energy will be larger than at later stages during the motion away from the surface.

In theories concerning total sputtering yields and kinetic energy distributions of sputtered particles, nuclear motion is always treated as motion of a classical particle along a classical trajectory, even though many of the sputtered particles have kinetic energies of fractions of an electron-volt. It is not obviously clear that that is permitted in sputtering events concerning excitations. However, in binary atomic collisions, the relevance of applying a classical picture to the nuclear motion has been discussed thoroughly, see, e.g., Refs. 17—20. It comes out that there is a striking empirical success for the classical description to hold far beyond the warranty of the conditions.[19]

It is in principle impossible to separate the decay from the creation of the excited state. Yu *et al.*[16] measured mean velocities of approximately 3×10^5 cm/s for sputtered, excited Ba atoms. With such velocities, and with a mean atomic lifetime of 10^{-8} s, the sputtered atoms will move approximately a distance of 3×10^4 nm away from the sputtering site during a mean life. Such a long distance will normally ensure that the excited atoms will be essentially free atoms at the time of the decay; interactions from the target will be greatly reduced at such distances. However, if the decay takes place before the interaction between the surface and the sputtered atom has ceased, the light emitted will not form sharp spectral lines, but broadened spectral features will occur instead. We mention in passing that such a broadening will introduce an error in deduction of velocity distributions from spectral line breadths, assuming that the broadening is caused by the Doppler effect.

In addition to considering the excitation process itself, a possible radiationless deexcitation has to be taken into account. Radiationless deexcitation of a sputtered, excited atom in the vicinity of a solid surface has been discussed several times in the literature, see, e.g., Refs. 3, 4, 10, 12, and 21. The necessary condition for a one-electron nonradiative deexcitation to occur is that the upper level of the excited, sputtered atom energetically coincides with an empty state in the conduction band of the solid metal. If this condition is fulfilled, the excited electron may jump back from the atom to the metal. This is a resonance ionization process. The one-electron radiationless deexcitation may be prohibited if the surface is oxidized because a band gap is then introduced in the solid. The possibility of a one-electron radiationless deexcitation to occur at clean metal surfaces, in combination with its disappearance when oxygen is present at the surface, has been used repeatedly to explain that atomic excitation probabilities in many cases increase rapidly when oxygen is admitted to the surface, see, e.g., Refs. 22—24. However, various shortcomings concerning radiationless deexcitation have been previously pointed out.[4,22,24] An alternative explanation for the enhancement of production of excited atoms caused by the presence of oxygen at the target surface has been suggested.[4,10,12] The idea is based on the above-mentioned fact that relaxation times are much longer for

oxygenated surfaces than for clean metals. Therefore, for clean metals, sputtered atoms will interact with a relaxed surface, whereas for surfaces containing oxygen, the sputtered atoms may interact with an excited surface, and this may naturally lead to larger excitation probabilities.

III. EXPERIMENTAL SETUP, DATA TREATMENT, AND RESULTS

The accelerator, the experimental equipment, and also the data treatment have been described previously,[1] so that only the essentials are mentioned below. Solid targets of elemental magnesium, aluminum, calcium, or cadmium (99.99% pure) were bombarded with 80 keV Ar^+ ions. The residual gas pressure in the target chamber was around 10^{-9} Torr, so that once the target surface had been cleaned because of the heavy ion bombardment, it stayed clean.

A quantum efficiency calibrated scanning monochromator[1] observed photons emitted from sputtered particles in the wavelength interval 170—1000 nm. The quantum efficiency calibration was performed with a deuterium lamp (170—400 nm) and a filament lamp (250—1000 nm). The two calibrations agreed where overlapping occurred. The observation region was a semicylinder of radius 2 cm, located around the beam spot on the target.[1] Such an observation geometry ensures that essentially all decays take place in the observation region, making a cascade correction possible in principle.[1]

With such a detection geometry, the relative population N_j' of level j (including all kinds of repopulations from upper levels decaying to level j) is given by[1]

$$N_j' = S(\lambda_{jk})/K(\lambda_{jk})b_{jk} \quad , \tag{1}$$

where $S(\lambda_{jk})$ is the signal of the optical transition from level j to level k at wavelength λ_{jk}, $K(\lambda_{jk})$ is the overall quantum efficiency of the detecting device, and b_{jk} is the branching ratio for the transition studied.

The relative population N_j of level j, corrected for cascade repopulations, is given by[1]

$$N_j = N_j' - \sum_i N_i' b_{ij} \quad , \tag{2}$$

where the summation has to be carried out over all levels i which decay to level j. A proper cascade correction can only be carried out when a sufficient number of upper levels are observed.

From Eqs. (1) and (2) it is readily seen that a prerequisite for a proper data treatment is knowledge about all branching ratios of relevance. For neutral alkali metals and alkali-metal-like ions (i.e., Mg II, Al III, Ca II, and Cd II) theoretical branching ratios can be calculated in the numerical Coulomb approximation,[25] and in many cases these are of sufficient accuracy. The situation is much more problematic for the neutral group-II elements (Mg I, Ca I, and Cd I) as well as for Al I and Al II. However, since only branching ratios calculated in the numerical Coulomb approximation were available, these data[26] were used.

In Al I, for the $4s\ ^2S$—$5p\ ^2P$ transition, the numerical Coulomb approximation does not work.[26] A value of 0.4 was used in the data evaluation for the branching ratio. For the terms of configurations $3s\,3p\,3d\ ^4P, ^4D$, and $3s\,3p4s\ ^4P$ in Al I, branching ratios of 1 have been used, because their decays to the low-lying $3s\,3p^2\ ^4P$ term were observed, and they can decay only to quartets due to spin conservation. However, the branching ratios actually may well be smaller than one.

The experimental results obtained with Mg, Al, and Ca are shown in Figs. 2—5. The cadmium data are not nearly as complete as those given in Figs. 2—5, and consequently, they are not presented in a figure.

The data given in Figs. 2—5 were treated for cascade repopulations in the following manner. For the neutral spectra, it comes out that the relative level populations decrease very steeply with increasing excitation energy, cf. Figs. 2, 3, and 5. This implies that cascade corrections are small in such cases, and therefore, populations uncorrected for cascades are given for Mg I, and Al I. As an example, in Al I, for the 4s term, a reasonably correct and complete cascade correction could be carried out (the population of the 4p term had to be extrapolated from the p-series populations). The ratio of the cascade corrected-to-uncorrected population is 0.86, in other words, the cascade repopulation is almost negligible. Since the p and f levels were not observed, the d levels could not be cascade corrected. As the correction to the 4s level is so small, and also because the 3d level could not be cascade corrected, only level populations uncorrected for cascades are presented for Al I. Cascade corrections for Mg I and Al I are of the order of the overall uncertainties of 10—20 % or smaller.

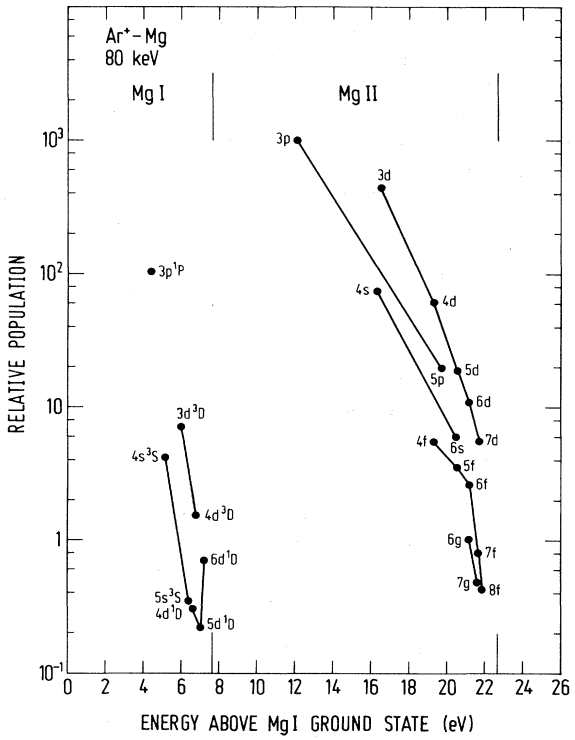

FIG. 2. Relative populations of some levels in Mg I and Mg II plotted vs the level excitation energy above the ground state in neutral magnesium. The Mg II data are cascade corrected, whereas the Mg I data are not; see text.

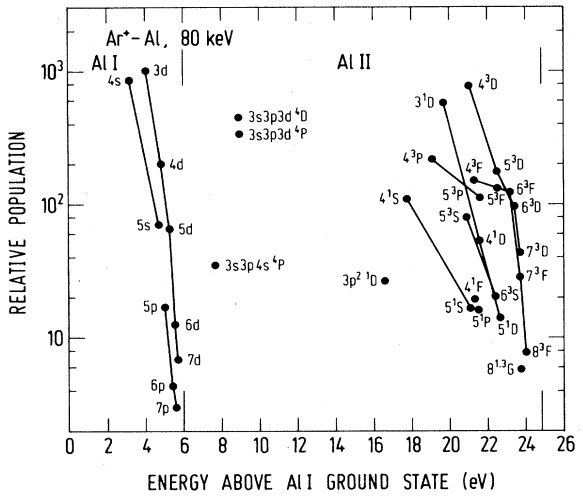

FIG. 3. Relative populations of some levels in Al I and Al II plotted vs the level excitation energy above the ground state in neutral aluminum. The data are uncorrected for cascades; see text.

For Mg II and Ca I detailed cascade corrections could be carried out, and the data presented are therefore cascade corrected. For the lowest-lying levels in Mg II, the corrections were as high as 30—40 %.

For Al II the data set is too sparse to permit a thorough cascade correction. Fortunately for Al II the situation is similar to that for the neutrals, namely that cascade effects are small. The data given are uncorrected for cascades.

Al III is a special and important case as we shall see. Therefore, we shall discuss cascade effects in detail for Al III. The level populations uncorrected for cascade effects are given in Fig. 4. As seen from that figure, the

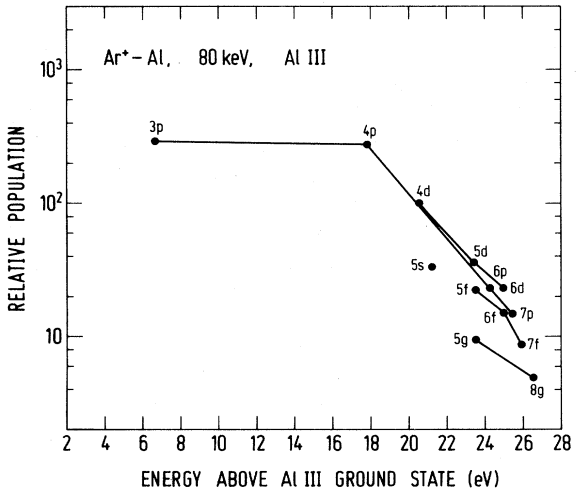

FIG. 4. Relative populations of some levels in Al III plotted vs the level excitation energy above the ground state in Al III. The data are uncorrected for cascades. For a detailed discussion of cascade effects see text.

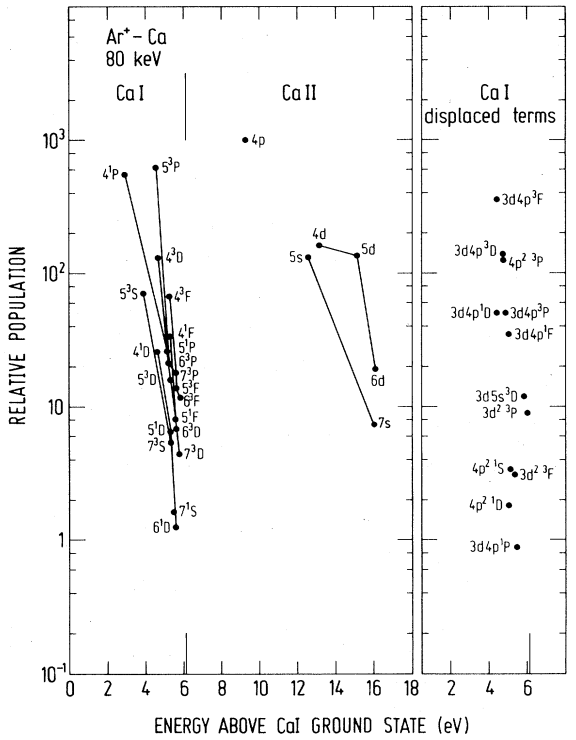

FIG. 5. Relative populations of some levels in Ca I and Ca II plotted vs the level excitation energy above the ground state in neutral calcium. The Ca I data are cascade corrected, whereas the Ca II data are not; see text.

data set is so incomplete that corrections can only be done incompletely, especially because the 3*d*- and 4*s*-level populations were not observed. Nonetheless, the cascade correction will be larger for the 3*p* level than for the 4*p* level. Therefore, since the uncorrected populations for these two levels are essentially equal, the corrected population for the 3*p* level must be lower than that for the 4*p* level. From extrapolations the corrected 4*p*-level population is estimated to be at least three times as large as that of the 3*p* level. In other words, for the *np* term series in Al III, an inverted level population is observed. This is most remarkable.

With magnesium, all transitions observed by us could be identified with confidence as previously observed, well-established transitions. For aluminum, identifications of two lines observed at 398.0 and 419.0 nm could be questioned. The lines can be identified as the 5*d*-8*f* and 5*f*-8*d* transitions in Al III, respectively. However, their intensities appeared as unreasonably large, yielding relative populations of 20 and 50, on the scale used in Fig. 4, for the 8*f* and 8*d* levels in Al III, respectively. The relatively strong intensity of the 5*d*-8*f* transition is in agreement with Braun,[22] who reported an even stronger relative signal than we have observed. His stronger relative signal can be explained from his detection geometry, since he used a lens to select only light from a very narrow region close to the surface.

With calcium and cadmium we observed fairly many lines which neither could be assigned to previously identified transitions nor to impurities (we observed in no case

expected impurities like sodium or any hydrocarbons). The lines are most presumably due to transitions from displaced terms in these two elements. The schemes of displaced terms are only incompletely known for calcium and cadmium.

IV. DISCUSSION

The electronic energy properties of solid Mg, Al, and Ca are in Figs. 6—8 shown (to the left) together with sections of the level schemes of the free atoms and ions of relevance. The ionization limits have been placed at the same level in all cases, so that electron binding energies are readily comparable. Work-function values have been taken from Ref. 27.

As outlined in Sec. II, the electronic energy properties of the solid can be expected to influence the distribution of excitation upon the different excited levels in the way that the electrons will tend to conserve their binding energy. Final levels which demand a relatively large amount of binding energy exchanged between the electron in question and the nuclear motion will be populated less than levels which have binding energies equal to, or close to, the binding energies of the valence electrons in the solid (remembering that level shifting and broadening will make the precise positions of the top and bottom of the valence band irrelevant). This expectation is generally in accordance with the experimental results given in Figs. 2—5. For all levels with binding energy smaller than the work function of the corresponding solid, we observe a rapid decrease in level population as a function of the level excitation energy. The only exception from this rule is the $6d\ ^1D$ level in Mg I. However, this level is known to have a strong configuration mixing with a displaced term, so that the pure LS-coupling label used in this work is not valid, and the relatively strong excitation observed here shall undoubtedly be explained in terms of configuration mixings.

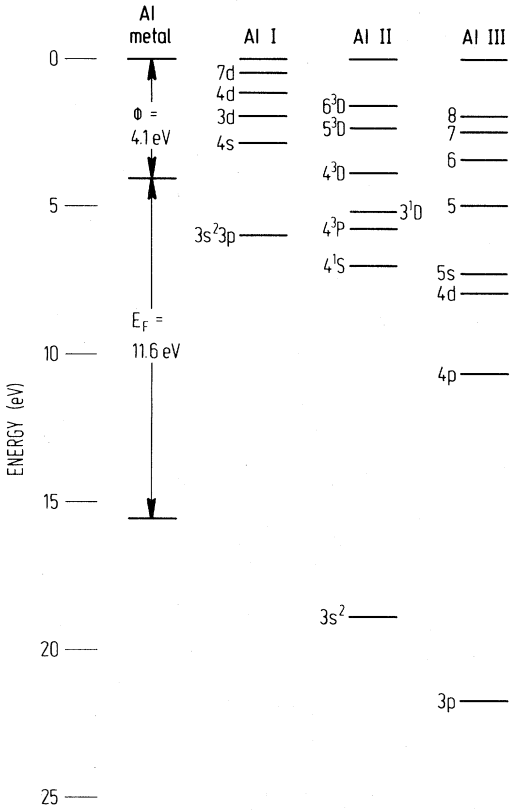

FIG. 7. Fermi level E_F and the work function ϕ of aluminum metal are shown together with the level energy diagrams for neutral aluminum (Al I), singly ionized aluminum (Al II), and doubly ionized aluminum (Al III). Note that the Al III 3s ground state has been omitted. The binding energy of the Al III 3s ground state is 28.4 eV.

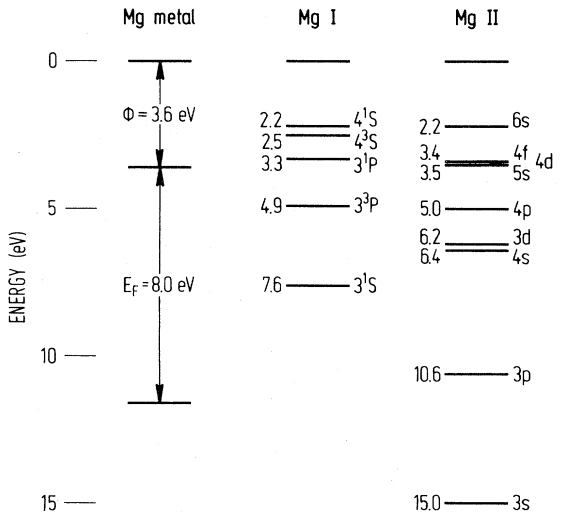

FIG. 6. Fermi level E_F and the work function ϕ of magnesium metal are shown together with the level energy diagrams for neutral magnesium (Mg I) and singly ionized magnesium (Mg II).

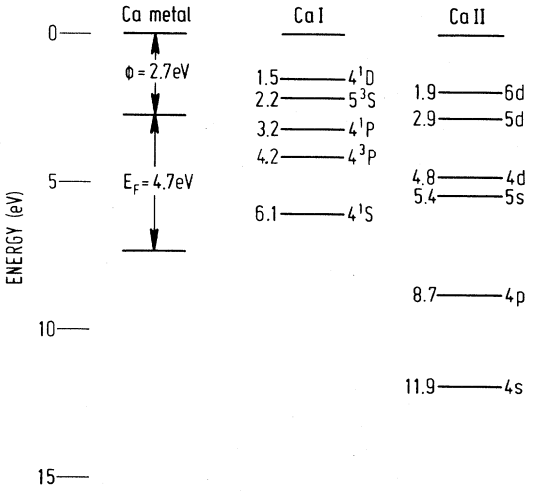

FIG. 8. Fermi level E_F and the work function ϕ of calcium metal are shown together with the level energy diagrams for neutral calcium (Ca I) and singly ionized calcium (Ca II).

The most remarkable result of the present investigation is the inverted level population observed for the p levels in Al III, namely that the cascade-corrected level population for the $3p$ level in Al III falls at least a factor of 3 below that for the $4p$ level, cf. Sec. III. Also, this finding can be understood from the expectation outlined in Sec. II that the electrons will tend to conserve their binding energy. As seen from Fig. 7, the $3p$ level in Al III has a binding energy of more than 6 eV *larger* than the most tightly bound electrons in the valence band of solid aluminum, and this large amount of change of binding energy undoubtedly causes the relatively small population of the $3p$ level in Al III.

We must mention here that the low population of the $3p$ level in Al III cannot be explained from one-electron radiationless deexcitations. This is because the $3p$ level has a binding energy larger than the bottom of the valence band of the solid, cf. Fig. 7. Only radiationless processes involving rearrangement of two or more electrons can take place for the $3p$ level. Such processes are much more rare than one-electron processes, and are most unlikely to occur, remembering that there has not yet been observed any direct indication of the presence of one-electron radiationless deexcitations in sputtering, cf. Sec. II.

There is a great qualitative similarity between the relative level population trends observed for Al I, II, and III (Figs. 3 and 4) and those observed for beam-foil excited C IV, N V, and O VI, see Fig. 1 in Ref. 28, which here is reproduced as Fig. 9. For Al I and C IV the level populations decrease quickly with increasing level excitation energy. For Al II and N V there is a shoulder in the level population data (similar shoulders are also seen in the Mg II and Ca II data, see Figs. 2 and 5), and for Al III and O VI we observe an inverted population for the lowest-lying levels. The results shown in Figs. 3 and 4 thus draw a strong parallel between the excitation mechanisms active in sputtering processes and in beam-foil interactions. The parallel is further demonstrated by comparing the inverted level population found here for Al III with the beam-foil level population data for Ar VIII and Kr VIII reported in Ref. 29.

From the level energy properties of calcium given in Fig. 8, one would expect a similar inverted population for the p levels in Ca II. Unfortunately, the Ca II data (Fig. 5) are too sparse to draw any conclusion. However, it can be said that a proper cascade correction would reduce the population of the $4p$ level in Ca II substantially. Indeed, it will fall somewhat below that of the $4p\ ^1P$ level in Ca I, and this is another important finding, because we have previously observed for other second-period elements that the ions are excited much more efficiently than the corresponding neutral atoms in sputtering.[2] The preferential excitation of the ions was explained[2] in terms of resonant electron pickup, a process which is excluded for the neutral atoms of the elements studied in Ref. 2. However, for calcium, according to Fig. 8, the $4p\ ^1P$ and the $4p\ ^3P$ levels of Ca I can be excited through resonant electron pickup processes which, on the other hand, are prohibited for the $4p$ level in Ca II. The $4p\ ^3P$ level in Ca I is metastable, so its population cannot be measured with our equipment. However, we find generally that the triplet levels are populated substantially above the corresponding singlets (generally a factor of 5 above). Thus, remembering the substantial reduction in population a cascade correction would imply for the $4p$ level in Ca II, we learn from Fig. 5 that for calcium the neutral atoms are excited much more efficiently than the ions are, contrary to what previously was found[2] for Be, Mg, Zn, and Cd. Indeed the difference in neutral-to-ion excitation ratios for Mg and Ca can be seen from Figs. 2 and 5, and is understandable from the binding-energy relations shown in Figs. 6 and 8. This finding can be regarded as a predictive test of the ideas outlined in Ref. 2, as well as being in accord with those given in Sec. II of this paper.

It is interesting to note that for neutral aluminum and calcium not only are the normal terms (of configurations $3s^2nl$ and $4snl$, respectively) excited, but also displaced terms are populated appreciably, cf. Figs. 3 and 5. For instance, the $3s\,3p\,3d$ configuration in Al I has a total population almost as large as those of the $4s$ or $3d$ levels, in spite of its high excitation energy of approximately 8.4 eV, see Fig. 3. This is in accordance with the independent-electron picture outlined in Sec. II. The electrons are transferred to their final orbitals independent of each oth-

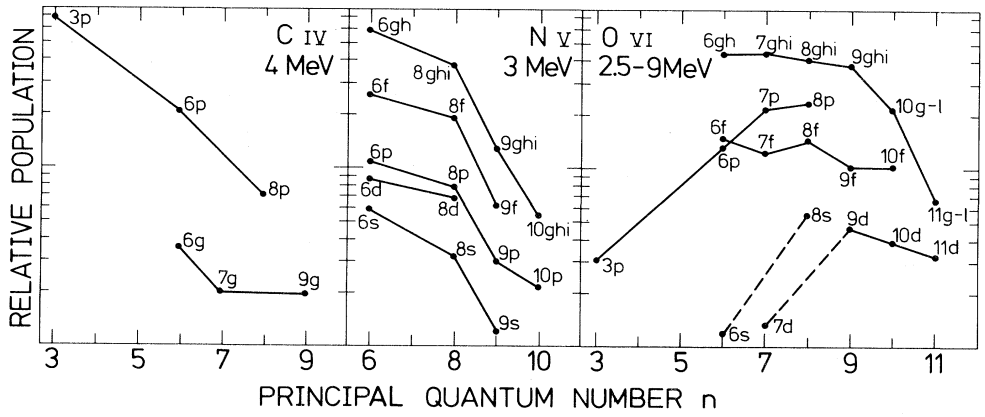

FIG. 9. Relative level populations for some terms in C IV, N V, and O VI (all of configuration $1s^2nl$) vs the principal quantum number of the excited level after beam-foil excitation. All relative level-population data for one element are on the same scale, whereas the scale changes from element to element. The figure has been taken from Ref. 28.

er, and consequently not only one, but more than one electron may end up in some excited orbital rather than in the ground state.

We wish to emphasize that whereas the strong populations of the high-lying displaced terms are in principle easily understood from the considerations given in Sec. II, such findings are not contained within the model given in Ref. 6.

It is remarkable to note that levels of high-spin multiplicity are preferentially populated when compared to corresponding levels of low-spin multiplicity. The triplets in Mg I, Al II, and Ca I are generally populated substantially more than three times above the corresponding singlets. Such deviations from statistical weight ratios are surprising because none of the targets applied here can have a magnetic structure. A tentative explanation has been given in Ref. 3 and shall therefore not be repeated here.

For Mg, Al, and Ca, no inner-shell excitations were observed, in agreement with the ideas outlined in Sec. II, because the inner-shell electrons are tightly bound in these elements. However, for cadmium, the outermost of the inner shells comes close in binding energy to the valence-shell electrons. The normal terms of Cd II are of configuration $4d^{10}nl$, but there are two levels, involving inner-shell excitation, of configuration $4d^9 5s^2\,{}^2D_{5/2}$ and $^2D_{3/2}$ which have excitation energies comparable to the lower-lying normal terms in Cd II. Of these two levels of configuration $4d^9 5s^2$ we observed a strong excitation of the $^2D_{5/2}$ level but not of the $^2D_{3/2}$ level. This is surprising, because normally, the different levels belonging to the same term are excited in ratios proportional to their statistical weights $2J+1$, but here the $^2D_{5/2}$ level was populated much over and above the $^2D_{3/2}$ level. This can be understood from the ideas outlined in Sec. II, together with the fact that for heavy elements, the distinct shell structure disappears gradually for the last outermost of the inner shells.[30] In solid cadmium the $4d\,{}^2D_{5/2}$ electrons have less binding energy than the $4d\,{}^2D_{3/2}$ electrons. There is a small probability that a $4d$ electron participates in the valence band. In such cases the core vacancy will be $^2D_{5/2}$ rather than $^2D_{3/2}$ owing to the different binding energies. Thus some of the sputtered cadmium atoms may initially have a $4d\,{}^2D_{5/2}$ vacancy but not a $4d\,{}^2D_{3/2}$ vacancy. Capture of two electrons to the $5s$ orbital during the sputtering event will lead to excitation of the $4d^9 5s^2\,{}^2D_{5/2}$ level, but not to the $^2D_{3/2}$ level, explaining our finding.

ACKNOWLEDGMENTS

The monochromator has been placed at our disposal by the Danish Natural Science Research Foundation, which we gratefully acknowledge. We also want to thank Mr. K. Jensen for skillful operation of the accelerator as well as for collecting data. Discussions with Dr. J. Nørskov are highly appreciated.

[1]N. Andersen, B. Andresen, and E. Veje, Radiat. Eff. 60, 119 (1982).
[2]E. Veje, Surf. Sci. 100, 533 (1981).
[3]E. Veje, Phys. Rev. B 28, 88 (1983).
[4]E. Veje, Surf. Sci. 109, L545 (1981).
[5]R. Kelly, in *Proceedings of the Third International Workshop on Inelastic Ion-Surface Collisions, Feldkirchen-Westerham, September, 1980,* edited by E. Taglauer and W. Heiland (Springer, Berlin, 1981), p. 292.
[6]R. Kelly, Phys. Rev. B 25, 700 (1982).
[7]See, e.g., *Sputtering by Particle Bombardment,* Vol. 47 of *Topics in Applied Physics,* edited by R. Behrish (Springer, Berlin, 1981).
[8]See, e.g., C. Kittel, *Introduction to Solid State Physics,* 4th ed. (Wiley, New York, 1971).
[9]See, e.g., M. Barat and W. Lichten, Phys. Rev. A 6, 211 (1972); J. S. Briggs, Rep. Prog. Phys. 39, 217 (1976).
[10]P. Williams, Appl. Surf. Sci. (in press).
[11]N. D. Lang and A. R. Williams, Phys. Rev. B 25, 2940 (1982).
[12]P. Williams, Surf. Sci. 90, 588 (1979).
[13]A. Sommerfeld, Naturwissenschaften 41, 825 (1927).
[14]E. Veje, Phys. Rev. A 14, 2077 (1976).
[15]R. E. Olson, Phys. Rev. A 24, 1726 (1981).
[16]M. L. Yu, D. Grischkowsky, and A. C. Balant, Phys. Rev. Lett. 48, 427 (1982).
[17]C. A. Coulson and K. Zalewski, Proc. R. Soc. London Ser. A 268, 437 (1962).
[18]S. A. Lebedeff, Phys. Rev. 165, 1399 (1968).
[19]J. B. Delos, W. R. Thorson, and S. K. Knudson, Phys. Rev. A 6, 709 (1972).
[20]J. B. Delos and W. R. Thorson, Phys. Rev. A 6, 720 (1972).
[21]H. D. Hagstrum, in *Electron and Ion Spectroscopy of Solids,* edited by L. Fiermans, J. Vennik, and W. Dekeyser (Plenum, London, 1978) p. 273.
[22]M. Braun, Phys. Scr. 19, 33 (1979).
[23]I. S. T. Tsong and S. Tsuji, Surf. Sci. 94, 269 (1980).
[24]C. M. Loxton, R. J. MacDonald, and P. J. Martin, Surf. Sci. 93, 84 (1980).
[25]A. Lindgård and S. E. Nielsen, At. Data Nucl. Data Tables 19, 533 (1977).
[26]A. Lindgård (unpublished).
[27]See, e.g., *American Institute of Physics Handbook,* edited by D. E. Gray (McGraw-Hill, New York, 1963).
[28]B. Andresen, B. Denne, J. O. Ekberg, L. Engström, S. Huldt, I. Martinson, and E. Veje, Phys. Rev. A 23, 479 (1981).
[29]S. Bashkin, H. Oona, and E. Veje, Phys. Rev. A 25, 417 (1982).
[30]R. J. Boyd, Phys. B 9, L69 (1976).